ELSEVIER

Journal of Structural Geology 28 (2006) 1734–1747

JOURNAL OF STRUCTURAL GEOLOGY

www.elsevier.com/locate/jsg

Analogue modelling of syntectonic leucosomes in migmatitic schists

Elena Druguet*, Jordi Carreras

Departament de Geologia, Universitat Autònoma de Barcelona, Unitat de Geotectònica, Edifici Cs, E-08193 Bellaterra (Barcelona), Spain

Received 28 February 2006; received in revised form 24 June 2006; accepted 30 June 2006
Available online 1 September 2006

Abstract

Migmatites from the Cap de Creus tectonometamorphic belt display a wide variety of structures, from those formed when the leucosomes were melt-bearing, to those developed during solid-state deformation. The observed field structures have been modelled by means of analogue experiments. The materials used in the models are layered plasticine as a schist analogue, and chocolate as analogue of the crystallizing leucosome. A model for the development of syntectonic migmatites is proposed in which initial melt-bearing patches, preferentially formed within fertile pelitic layers, progressively evolve towards lens-shaped veins. Furthermore, heterogeneous deformation of anisotropic metasediments facilitates formation of extensional sites for further melt accumulation and transport. Melt crystallization implies a rapid increase in effective viscosity of leucosomes producing a reversal in competence contrast with respect to the enclosing schists. During the whole process, deformation localizes around crystallizing veins, giving rise to different and contrasting structures for melt-bearing and for solid-state stages.

Keywords: Analogue modelling; Deformation; Melt; Migmatite; Rheology

1. Introduction

Partial melting and deformation are spatially- and temporally-related processes. This is because deformation under any tectonic regime increases melt mobility and facilitates the space for melt accumulation, transport and final emplacement (Hutton, 1988; D'Lemos et al., 1992; Brown, 1994; and numerous articles in Bouchez et al., 1997; Benn et al., 1998 and Castro et al., 1999). Furthermore, there is much evidence for melt controlled strain localization (McLellan, 1984; Hollister and Crawford, 1986; Davidson et al., 1994; Grujic and Mancktelow, 1998). This double cause-and-effect framework provides the feedback relations between migmatization (or broad magmatic processes) and deformation (Brown and Solar, 1998; Brown, 2004).

Crystallization of migmatitic veins implies a dramatic increase in partial melt viscosity controlled by the volume fraction of melt in the solid-liquid aggregate. Since the work of Arzi (1978), this drastic rheological change has been studied by theoretical and experimental means, being a subject of long-standing debate in petrology and structural geology (see review in Rosenberg and Handy, 2005, and references therein). However, its consequences concerning strain localization and development of structures related to syntectonic migmatites at different scales have been comparatively less investigated (McLellan, 1984; Brown and Solar, 1998). In the present study particular attention is given to whether these rheological changes are in turn reflected in changes in geometry and fabrics.

We explore the structural patterns displayed in syntectonic leucosomes and in the adjacent host mesosome in order to gain knowledge of the deformation and rheologic factors involved in their development. This is a necessary approach, since migmatite structures are often used as tools for resolving the physical mechanisms that produce melt migration and emplacement and for determination of strain, kinematics and tectonic regimes. For this purpose, a combination of field and experimental methods has been adopted. Field observations in migmatitic outcrops from the Cap de Creus massif (Variscan of the eastern Pyrenees) were essential for recognising the

* Corresponding author. Tel.: +34 9 3581 1163; fax: +34 9 3581 1263.
E-mail address: elena.druguet@uab.es (E. Druguet).

0191-8141/$ - see front matter © 2006 Elsevier Ltd. All rights reserved.
doi:10.1016/j.jsg.2006.06.015

initial geometries of leucosomes and to get first insights into how are they modified to accommodate deformation. These natural features were afterwards modelled by means of a series of analogue experiments. The experimental results are highly consistent with field hypothese and, moreover, provide more clues on the development of syntectonic migmatites.

2. Field observations at Cap de Creus

Variscan LP/HT metamorphism, magmatism and migmatization in the Cap de Creus (eastern Pyrenees) are syntectonic with transpressional deformation. This has been largely verified in previous works (Druguet and Hutton, 1998; Druguet, 2001). The studied area is formed by locally migmatized upper amphibolite facies schists together with small granitoid bodies and a swarm of anatectic pegmatites (Fig. 1). Deformation displays a heterogeneous distribution, producing a km-scale sub-vertical E-W trending zone of high strain with a steep extension direction (Druguet et al., 1997; Druguet, 2001). The migmatitic schists which are the object of this study occur in two broad domains with regard to deformation gradients. One is a domain of relative low strain where partial melting is only incipient. The other is the high strain domain, which includes zones of incipient partial melting but also zones of pervasive migmatization and igneous activity (the so-called Cap Gros, Serena, Punta dels Farallons and Tudela migmatite complexes, Fig. 1). The migmatitic schists display distinctive features in these two domains as regard to occurrence, geometry and deformation structures, which will be described in next sections.

2.1. Structures in domains of relative low strain and incipient partial melting

In these domains, alternating sub-vertical layers of metagreywackes and metapelites form the predominant lithology. The main foliation (here S_1) is sub-parallel to bedding and more penetrative in the pelitic layers. S_1 is a result of the D_1 deformational event, which took place at the earliest stages of the Variscan metamorphism (Druguet, 2001). Although folded and crenulated to variable degrees during D_2 transpressional deformation which developed at peak-metamorphic conditions, the bedding-S_1 fabric is not completely transposed so that it defines the main anisotropy.

Small isolated leucosome patches appear systematically in the pelitic layers (Fig. 2), suggesting the local onset of partial melting in relatively more fertile layers (i.e. those with the more suitable composition for generating an anatectic melt). The grain size of the leucosomes varies between 0.5 and 8 mm and their composition varies from leucogranitic to trondhjemitic (Druguet et al., 1995), with quartz-plagioclase ± K-feldspar ± cordierite ± almandine as the main mineral assemblage.

In sections perpendicular to layering, individual leucosomes have a sub-circular (Fig. 2a), lenticular or very irregular, patchy (Fig. 2b) shape. They are generally more elongate

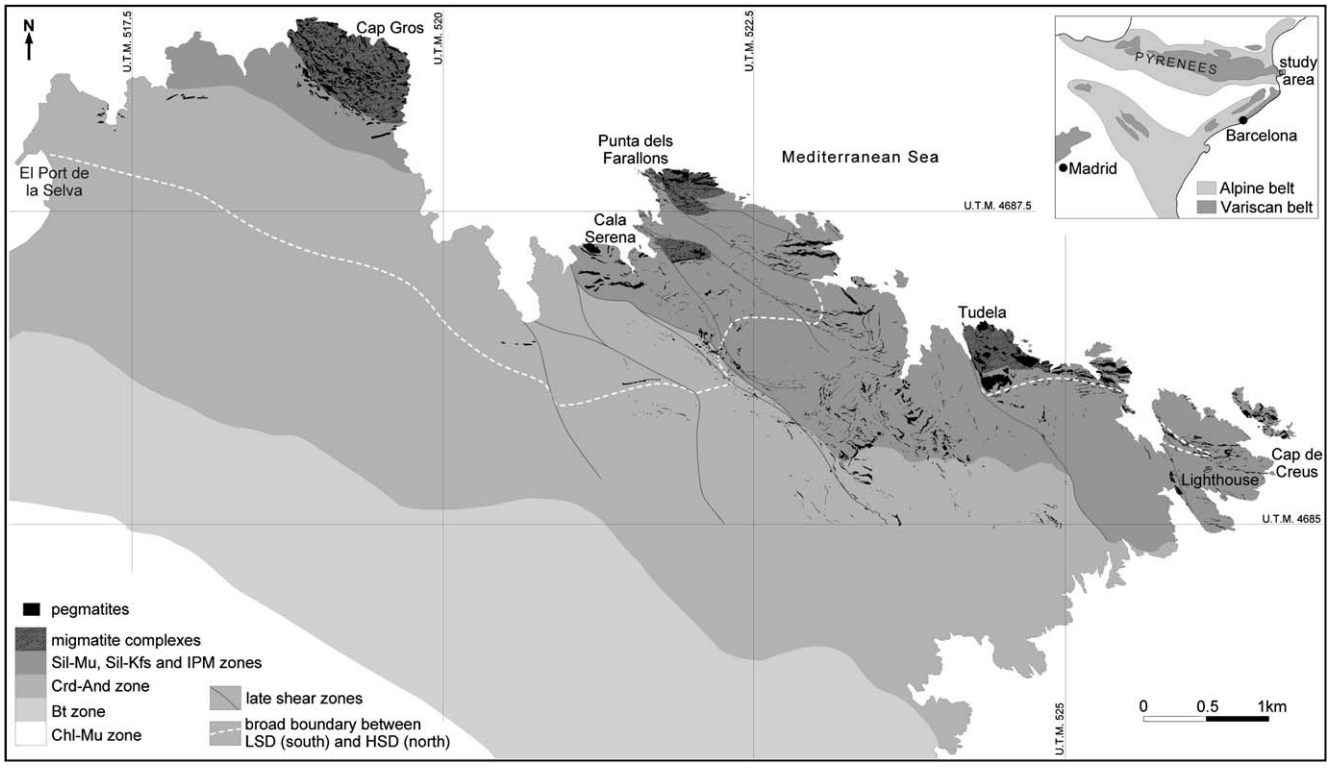

Fig. 1. Simplified map of metamorphic and migmatitic zones in the NE Cap de Creus tectonometamorphic belt (after Ramírez, 1983; Druguet and Hutton, 1998; Druguet, 2001). Abbreviations: Chl = chlorite, Mu = muscovite, Bt = biotite, Crd = cordierite, And = andalusite, Sil = sillimanite, Kfs = potassium feldspar, IPM = incipient partial melting, LSD = low strain domain, HSD = high strain domain. The curved shape of the boundary between the LSD and the HSD is a result of post-D_2 folding and shearing.

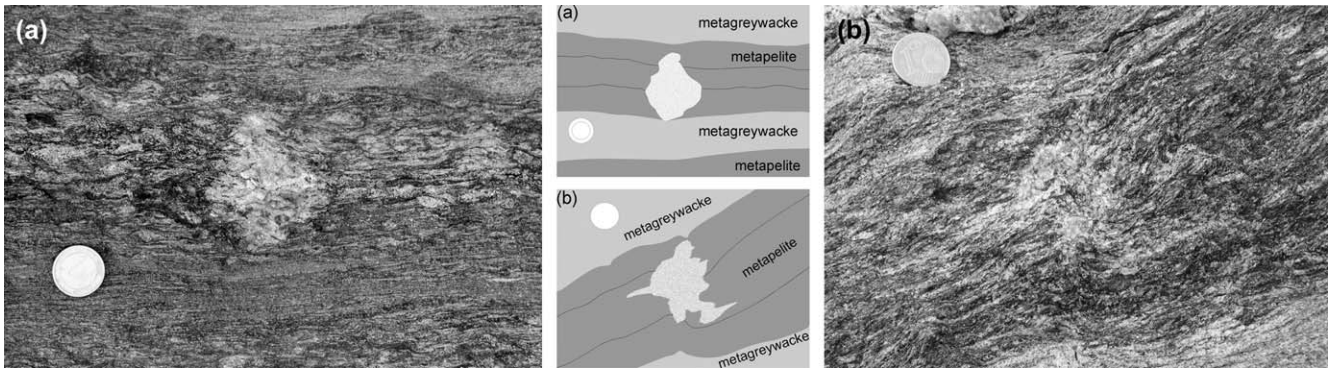

Fig. 2. Field photographs and related sketches of isolated leucosome patches from low strain domains. (a) Discordant, almost circular, pegmatitic patch developed in a pelitic layer (Lighthouse area). Section is sub-perpendicular to the stretching lineation. Width of view 23 cm. (b) Discordant diffuse leucocratic patch developed in a pelitic layer and showing a weak foliation necking effect (southeast of Cala Serena). Section is sub-parallel to the stretching lineation. Width of view 14 cm.

in sections perpendicular to layering and sub-parallel to the L_2 stretching lineation, such that leucosomes have a three-dimensional roughly fusiform shape. In all cases their occurrence is markedly discordant with layering.

Deflection of bedding-S_1 around discordant leucosomes is another common feature in this zone. In Fig. 2b, the schistosity in the pelitic layer around the leucocratic patch and the interphase pelite-greywacke are slightly deflected. This type of structure has been observed in a range of strain intensities from less to more deformed. In Fig. 3a metapelitic segments are pinched adjacent to the leucosomes, such that the structures resemble leucosome-filled interboudin partitions. Incipient leucosome patches are associated with incipient necking (detail shown in Fig. 3b) and larger patches are in turn usually linked with more marked necking (detail shown in Fig. 3c). This structure will be named ''foliation necking effect''.

There are numerous examples of similar structures in the literature, found in migmatite areas (Ramberg, 1955; Kisters et al., 1998; Grujic and Mancktelow, 1998, their Fig. 5a; Ghosh and Sengupta, 1999, their Fig. 5f; Vanderhaeghe, 1999, his Fig. 4g; Bons, 1999; Labrousse et al., 2002, their Fig. 4d; Marchildon and Brown, 2003, their Fig. 4b; Brown, 2004, his Fig. 2) but also around quartz or calcite veins from lower grade terrains (Lacassin, 1988; Swanson, 1992). The classical interpretation is that these structures result from layer or foliation boudinage, with veins occupying the interboudin partitions (necks, fractures). This is a reliable assessment for areas of pervasive boudinage where boudins develop in infertile layers of resistant material (e.g. amphibolite, calc-silicate rock). However, in the Cap de Creus, strain localization around soft, partially molten, material is envisaged as the main process responsible for the pinching of foliation. Thus, the foliation necking effect does not necessarily correspond to boudinage but it is the main way for a system with a strong mechanical contrast (molten material and schists) to accommodate deformation. The main evidence supporting this interpretation are:

(1) Leucosome patches are restricted to pelitic layers (Figs. 2 and 3), suggesting that sites of initial melting were controlled by lithology and that subsequent segregation and accumulation processes were constrained to the pelitic protolith.
(2) The presence in outcrops that are located close to each other of a gradient of structures, from small circular blobs to patches bounded by foliation necking patterns (Figs. 2 and 3).
(3) No foliation necking patterns or boudins are observed in layers without leucosomes and far away from these. In fact, the competence contrast between metapelitic and metagreywackic layers during D_2 deformation is considered to be low, the metagreywackes being slightly stiffer. This is probably because the greater amount of quartz in the greywackes is balanced by the coarser grains in the metapelites (due to more profuse porphyroblast growth) but without evidence of a strength reversal such as that described in some other high-grade metamorphic areas (e.g. Vernon et al., 2003).
(4) The regional maximum stretch is close to 1 in horizontal sections from low to medium strain domains where many of the described structures are found, and pegmatites emplaced at a low angle to the XY plane of finite strain are not boudinaged and may even be slightly shortened (Bons et al., 2004).

Progressive deformation in the solid-state (i.e. after full crystallization of melt-bearing patches) may lead to modification of former structures. This is suggested by the presence of some isolated leucosomes showing a lensoid shape subconcordant with layering. Also the foliation necking effect is overprinted by the opposite effect of viscous flow around leucosomes, hereafter named ''foliation wrapping effect''. Leucosomes at this stage represent competent inclusions with regard to the enclosing schists. An example of a leucosome which shows evidence of having been weakly deformed in the solid state is depicted in Fig. 3d.

2.2. Structures in the high strain domain

The domain of relative high D_2 strain is characterized by close to isoclinal folds of bedding-S_1 and a penetrative S_2

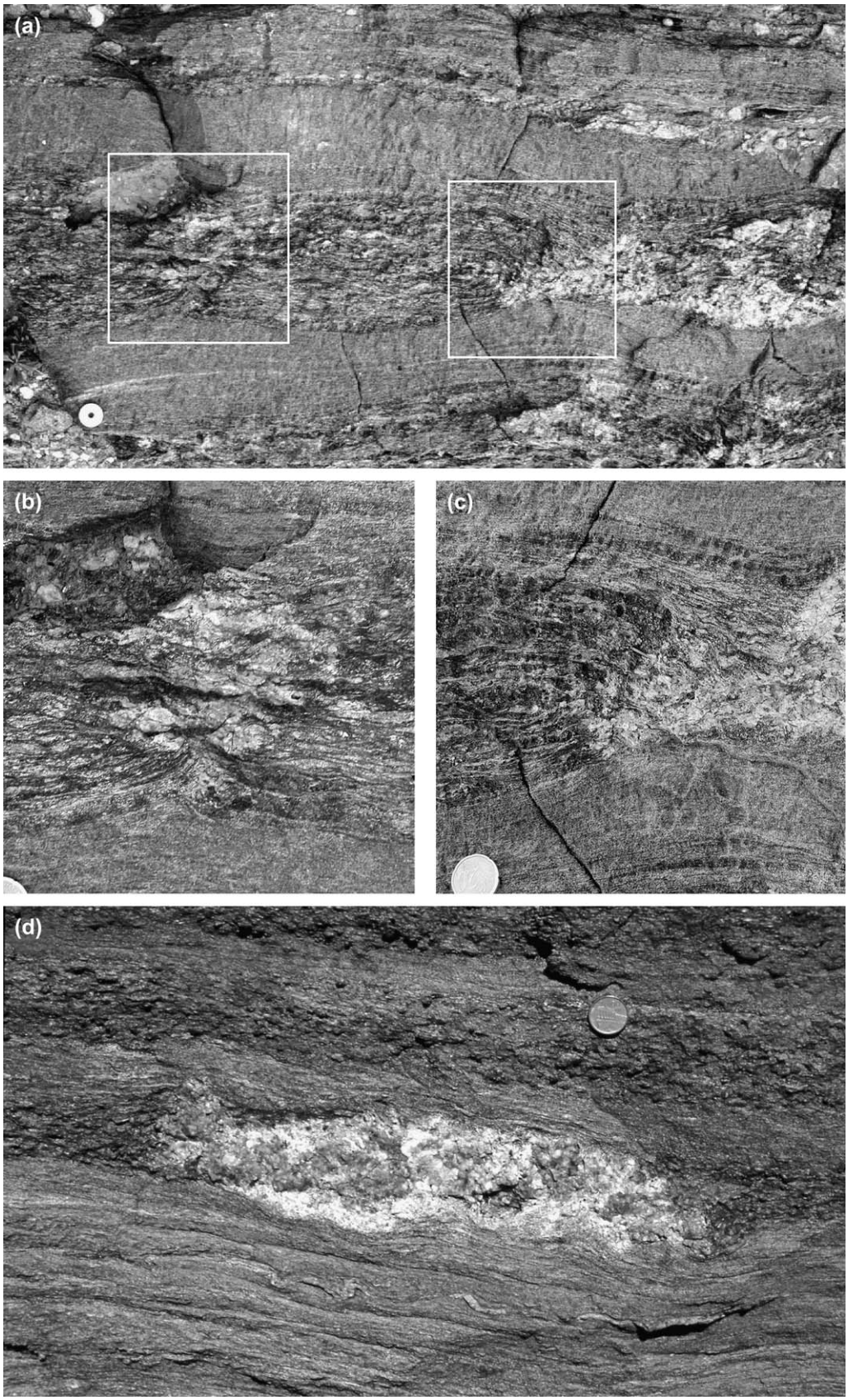

Fig. 3. Photographs of deformed leucosome patches and schists from the Lighthouse area. Outcrop surfaces are sub-perpendicular to the stretching lineation. (a) Discordant patches developed in a pelitic layer. There is a necking effect of foliation adjacent to leucosomes and weak solid-state stretching of the patches themselves. Note that the surrounding metagreywackes are less deformed. Width of view 66 cm. (b) and (c) Close-up views of the structures shown in (a). (d) Isolated pegmatitic leucosome showing a lensoid shape, sub-concordant with layering in the surrounding pelitic schists. Width of view 45 cm.

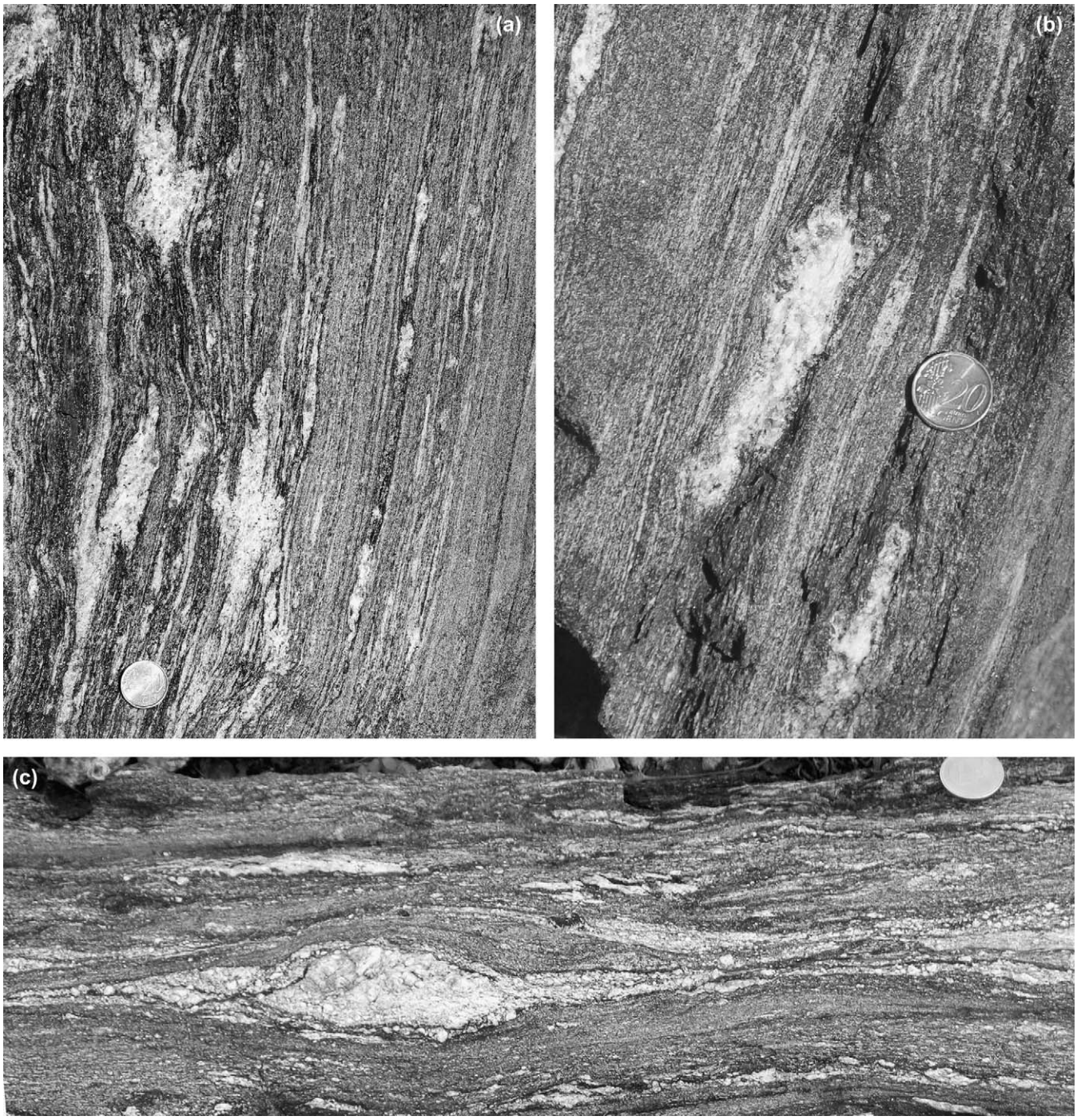

Fig. 4. Field photographs of deformed leucosomes. (a) Sub-concordant and concordant leucosomes are preferentially developed in pelitic layers. Note the development of some foliation wrapping effect, more marked in the small lenses at the right of the photograph. Section is sub-parallel to the stretching lineation. Width of view 24 cm. (b) Detail of a sub-concordant lens-shaped vein probably developed by subsequent solid-state deformation of a discordant patch. Section is sub-parallel to the stretching lineation. Width of view 14 cm. (c) Stromatic migmatite with some lens-shaped leucosomes. Section is sub-perpendicular to the stretching lineation. Width of view 33 cm. (a) and (b) are from the Tudela migmatite complex, and (c) is from the Cala Serena migmatite complex.

axial planar foliation. In consequence, the layering defined by bedding-S_1 is less recognisable due to D_2 transposition. Migmatites in this domain range from schists with isolated leucosome patches (in zones of incipient partial melting) to more widespread stromatic and nebulitic migmatites (in the migmatite complexes).

In zones of only incipient partial melting, leucosomes are restricted to the here transposed metapelitic layers. They exhibit foliation necking patterns developed prior to full crystallization of melt which are similar although generally more marked with increasing strain than those described above for the low strain domains.

In the migmatite complexes, which are restricted to the high strain domain, leucosomes are more abundant than in domains of incipient partial melting. Owing to D_2 transposition and pervasive migmatization, a new migmatitic layering is in general well developed, with alternating irregular bands of leucosome, melanosome and mesosome (Fig. 4a,c). Leucosomes rarely occur as isolated bodies, but as a series of patches, lenses or veins. Moreover, several generations of leucosomes have been recognised on the basis of structural and crosscutting criteria with regard to the main migmatitic layering. Leucosome patches also exhibit foliation necking patterns. However, they have more irregular shapes, with veins emanating from central pods and cross-cutting the migmatitic banding. These often leads to the development of complex vein networks consisting of cracks and discrete shear domains filled with leucosome (Fig. 5a) which resemble the diktyonitic structures described by McLellan (1988) or the interconnected leucosome networks of Brown and Solar (1999).

Often, leucosomes may have recorded deformation in the solid state, as shown by lenses stretched to different degrees towards parallelism with layering (Fig. 4b,c and Fig. 6). In this situation, the foliation wrapping patterns developed in solid-state conditions prevail over relics of foliation necking patterns. Also due to solid-state deformation, veins initiated at a high angle to layering (i.e. the leucosome-filled fractures) may subsequently become folded (Fig. 5b).

Hence, the structures present in both low and high strain domains suggest a syn-deformational reversal in competence contrast between leucosomes and schists. There is a range of structures around leucosomes whose end members are: (i) foliation necking effect, developed in a partial molten state of the leucosomes; and (ii) foliation wrapping effect, developed during solid-state deformation conditions. Their distinction is of particular interest because it may provide information on the changes in rheological and deformational behaviour of melt – host rock systems during the transition from partial melting to crystallization. The next section deals with these aspects through experimental approaches.

3. Analogue modelling

The aim of the experimental part of this work is to model the structures observed in the field and to test the hypothesis on the development of syntectonic leucosomes. The experiments were performed using the deformation apparatus BCN-stage, a strain rate controlled prototype which allows variable temperature operation (Carreras et al., 2000a).

Previous work by other authors on analogue modelling of partial melts and magmas include microstructural models to analyse the effect of liquid fraction on the deformation mechanisms at the grain-scale and to gain understanding on melt migration and segregation processes (Means and Park, 1994; Park and Means, 1996; Rosenberg and Handy, 2000; Walte et al., 2005). In their experiments, organic crystalline compounds, such as norcamphor, were used as analogues for the solid phases and different liquid compounds as melt analogues. Other experiments focused on melt segregation and ascent have used diverse melt analogues, such as in situ fermentation gas in wet sand (Bons et al., 2001) or partially molten waxes (Barraud et al., 2004). Grujic and Mancktelow (1998) explored the influence of weak inclusions (vaseline in a matrix of paraffin wax) in shear domain development. At larger scales, magma ascent processes (diapirism and dyking) and pluton emplacement have been extensively modelled since the famous work by Ramberg (1967). Among more recent studies which have modelled syntectonic intrusions are those by Román-Berdiel et al. (1997) whose experiments were based on the injection of a low viscosity silicone putty into a sand pack, and Galland et al. (2003) who used vegetable oil as magma analogue.

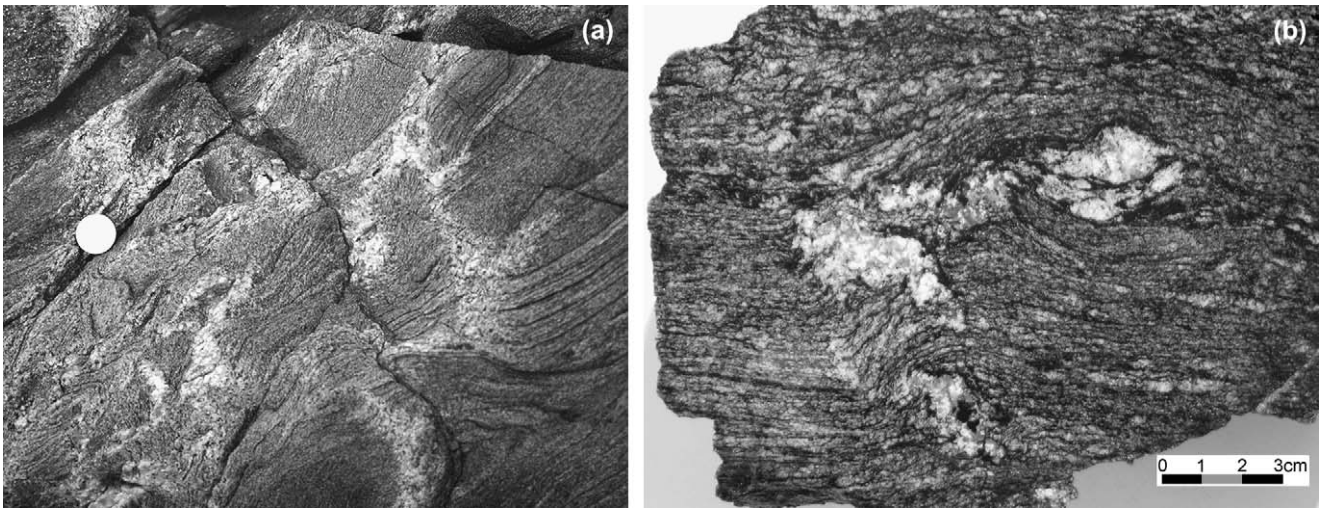

Fig. 5. Field photographs of migmatite structures from the Cala Serena migmatite complex. (a) Network of irregular patches interconnected throughout leucosome-filled fractures. Section is oblique to the stretching lineation. Width of view 28 cm. (b) Photograph of a hand specimen showing a folded and stretched leucosome vein. Note the presence of both foliation necking and foliation wrapping effects in the adjacent schist. Section is normal to the stretching lineation.

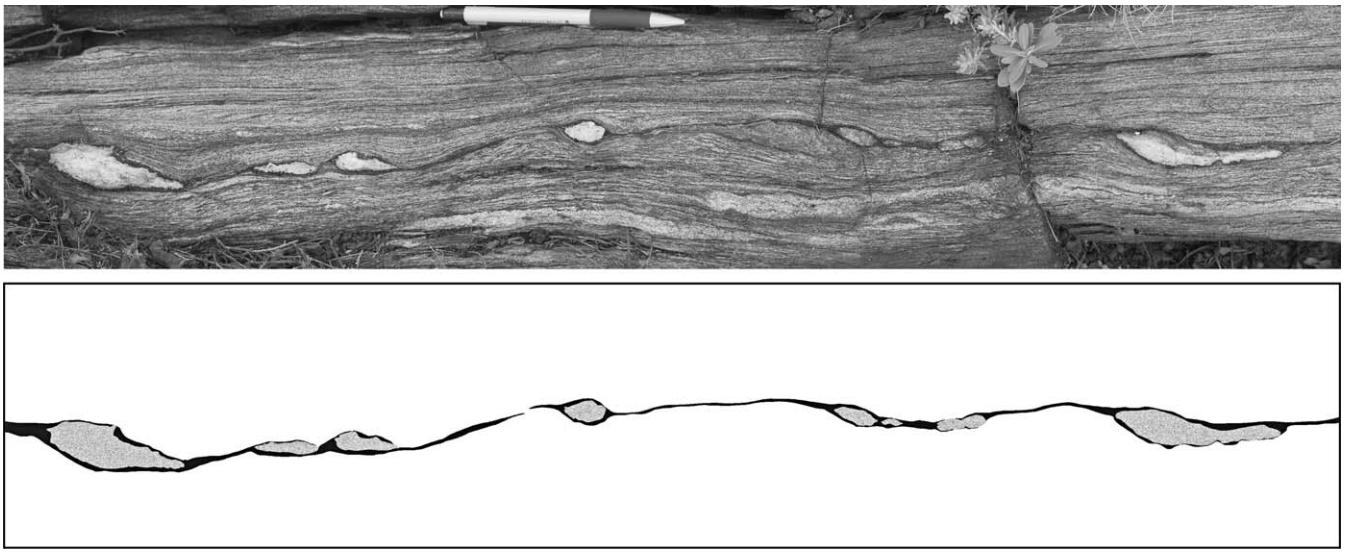

Fig. 6. Photograph and sketch of leucosome lenses within a stretched melanosome layer (Cala Serena migmatite complex). Outcrop surface is sub-parallel to the stretching lineation. Pencil for scale is 15 cm long. Note the strong foliation wrapping effect. Boudinage is partly apparent. Incorrect assumption of boudinage of an initially tabular leucosome vein would give around 200% extension parallel to foliation.

3.1. Analogue materials

As the present study focuses on structures developed in both the leucosomes and the schists at the transition from melt-bearing to solid-state system, we have investigated analogue materials to represent: (i) the ductile flow of anisotropic/layered rocks; and (ii) the deformational behaviour of a crystallizing melt.

A plasticine-vaseline-confetti mixture as an analogue of the schists: we used plasticine (from the company Oclu-Plast S.A., Barcelona) and 9 wt.% vaseline. This mixture was made anisotropic by adding paper flakes (confetti) in different proportions. Carreras et al. (2000b) and Gómez-Rivas et al. (2005) used similar mixtures to model shear domain development in anisotropic materials. Plasticine, a non-linear elastoviscous material, has been widely used as viscous rock analogue and its rheological properties are well established (McClay, 1976; Zulauf and Zulauf, 2004 and references within).

Chocolate as an analogue of the crystallizing melt: chocolate is a multiphase suspension based on cocoa butter, sugar and other minor particles. Largely because of its interest to the food industry, the rheology of chocolate is a matter of scientific investigation. It is also an ideal material for research into the effects of crystallization and liquid-solid phase change. Molten chocolate (36–38 °C) can be idealized as a Bingham plastic to a pseudoplastic fluid (Shackleton and Green, 1993; Beckett, 2000). Below 20–25 °C cocoa butter (which is the melt fraction in chocolate) crystallizes and chocolate behaves as a crystalline solid.

> Chocolate is a solid at room temperature, but melts into a smooth viscous liquid at body temperature (“melts in your mouth, …”). What other food has this property? I can’t think of any (Kovac, 2002).

Its low melting temperature and low temperature interval for phase change are in the range of temperatures of the experimental device used in this work. Moreover, its viscoplastic-Bingham behaviour fits with the rheology of most crustal partial melts (Petford, 2003). At the solid state, chocolate behaves more rigidly than plasticine, as do granitic veins which are usually more competent than their metamorphic host rocks. Despite substantial differences in crystallization process compared to silicate melts, the described properties make chocolate an appropriate analogue of crystallizing melt for the purpose of this study. This work represents the first attempt to use chocolate in experimental geology. For the experiments we used commercial dark couverture chocolate tablets.

Average values of viscosity in nature for both leucosomes and schists and their equivalent analogues for the experiments are detailed in Table 1.

Table 1
Values of strain rates and effective viscosities of mid crustal materials and their analogues used in the experiments

Parameter	Strain rate	Viscosity of host	Viscosity of partial melt	Viscosity of solid vein
Mid crust	10^{-14} s^{-1}	10^{18}–10^{19} Pa s (schist at 700–500 °C)	10^{5}–10^{12} Pa s (granitic melt at 700 °C)	10^{20}–10^{21} Pa s (granitic vein at 500 °C)
Laboratory	2.5×10^{-5} s^{-1}	10^{7} Pa s (plasticine)	2–60 Pa s (molten chocolate)	10^{10}–10^{12} Pa s (solid chocolate)

The strain rate value for the mid crust is taken from Pfiffner and Ramsay (1982). Viscosity values are taken from Davidson et al. (1994) for schists, Petford (2003) for granitic melts and rocks, Gómez-Rivas et al. (2005) for plasticine and Shackleton and Green (1993) for molten chocolate, and extrapolated from data in Barnes (1999) for solid chocolate.

3.2. Model design and deformation conditions

All models consist of 5 mm thick layers of anisotropic plasticine mixture. These layers were assembled in groups of low anisotropy plasticine (grey plasticine layers with 4.3 wt.% confetti) and high anisotropy plasticine (white plasticine layers with 12 wt.% confetti), to represent a cm-alternance of greywacke and pelitic schists respectively (Fig. 7). The resulting effective viscosity contrast between high and low anisotropic layers is very low, ~2 (Gómez-Rivas et al., 2005), the high anisotropic layers being slightly more viscous due to their higher confetti fraction.

In the high anisotropic layers, several (4 or 6) holes were perforated with the geometry of cylinders and rectangular prisms. The holes were subsequently filled with molten chocolate (melted over a bain-marie) before the start of the experiment (Fig. 7). The chocolate filled cavities represent melt accumulations in the fertile pelitic layers. Former processes of melt segregation ± migration were omitted in these models.

The experiments were performed under pure shear, plane strain boundary conditions at a constant strain rate of $2.5 \times 10^{-5}\ s^{-1}$, most under layer normal shortening (Figs. 7–10 and 11a) and some under layer parallel shortening (Fig. 11b). The cylindrical three-dimensional geometries of the chocolate-filled holes were adopted for simplicity in view of the limitations of the experiments to plane-strain conditions. All experiments were run at decreasing temperature although at different thermal conditions by varying initial (T_0) and final (T_f) cell temperatures. Experiments can be grouped into three main sets according to cooling rates: low ($T_0 = 28\ °C$; $T_f = 26\ °C$), intermediate ($T_0 = 28\ °C$; $T_f = 20\ °C$) and high ($T_0 = 23\ °C$; $T_f = 20\ °C$) cooling rate experiments. Temperature of molten chocolate at the onset of deformation was constant circa 38 °C. Details on experimental parameters important for the scaling of the models are given in Table 1.

A bulk finite strain axial ratio $R_{X/Z} = 4$ (50% shortening along Z axis) was attained in all tests in a time interval between 7 and 8 h. Photographs of the upper surface of the models were taken at 10 min intervals. At the end of the experiments, the deformed models were cut into 1 cm thick slices perpendicular to layering and scanned.

4. Modelling results

Interpretation of the modelling results is based on two procedures. One is the analysis of photographs taken at different deformation stages (Figs. 8 and 9) to construct the deformational history of individual experiments and to compare the results of different experiments. The second approach comprises the analysis of finite structures from different scanned slices (Figs. 10 and 11). This allows a more detailed examination of the developed structures and also the detection of possible internal variations.

4.1. Experiments under layer/foliation normal shortening

From the first strain increments, deformation concentrates around melt inclusions (molten chocolate). This is shown in Fig. 8 which illustrates four strain stages of an experiment

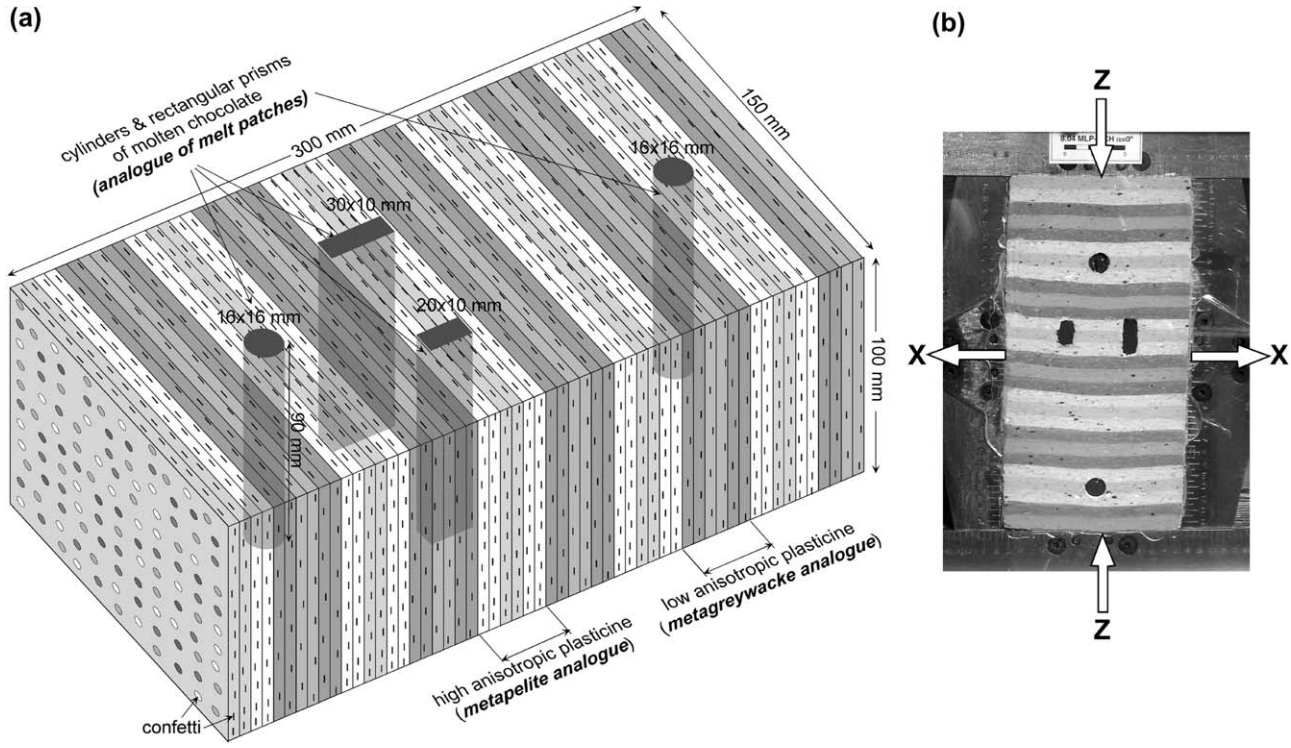

Fig. 7. (a) Sketch of a model used for experimental deformation under layer normal shortening. Models prepared to deform under layer parallel shortening differ from this in orientation of the layers at 90°. (b) Photograph of the upper surface of a model specimen at the onset of an experiment under layer normal shortening.

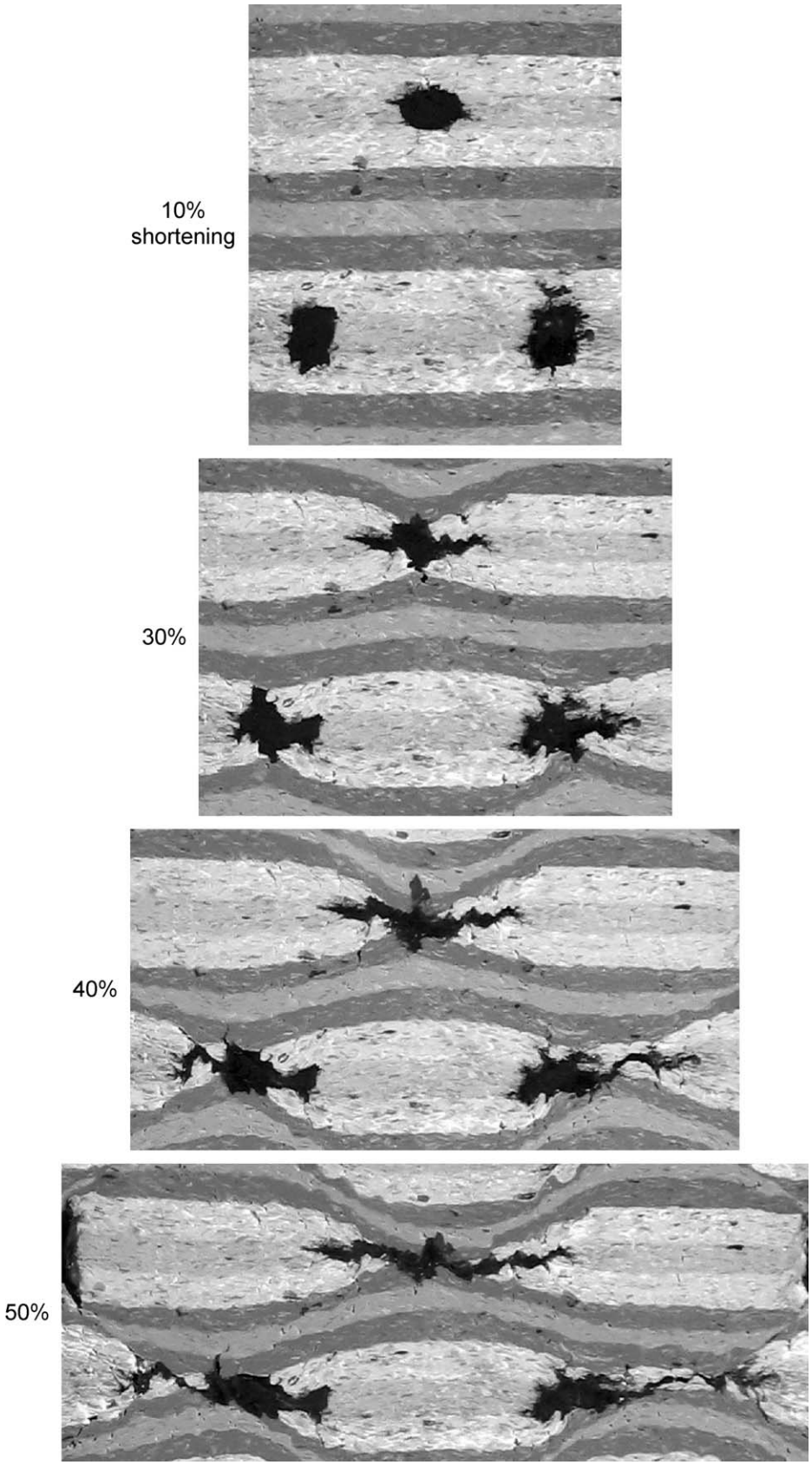

Fig. 8. Photographs of four deformation stages of an experiment performed under layer normal shortening and intermediate cooling rate. Note the progressive change in shape of the molten phase and the development of foliation necking effect in the layered matrix (see text for further description).

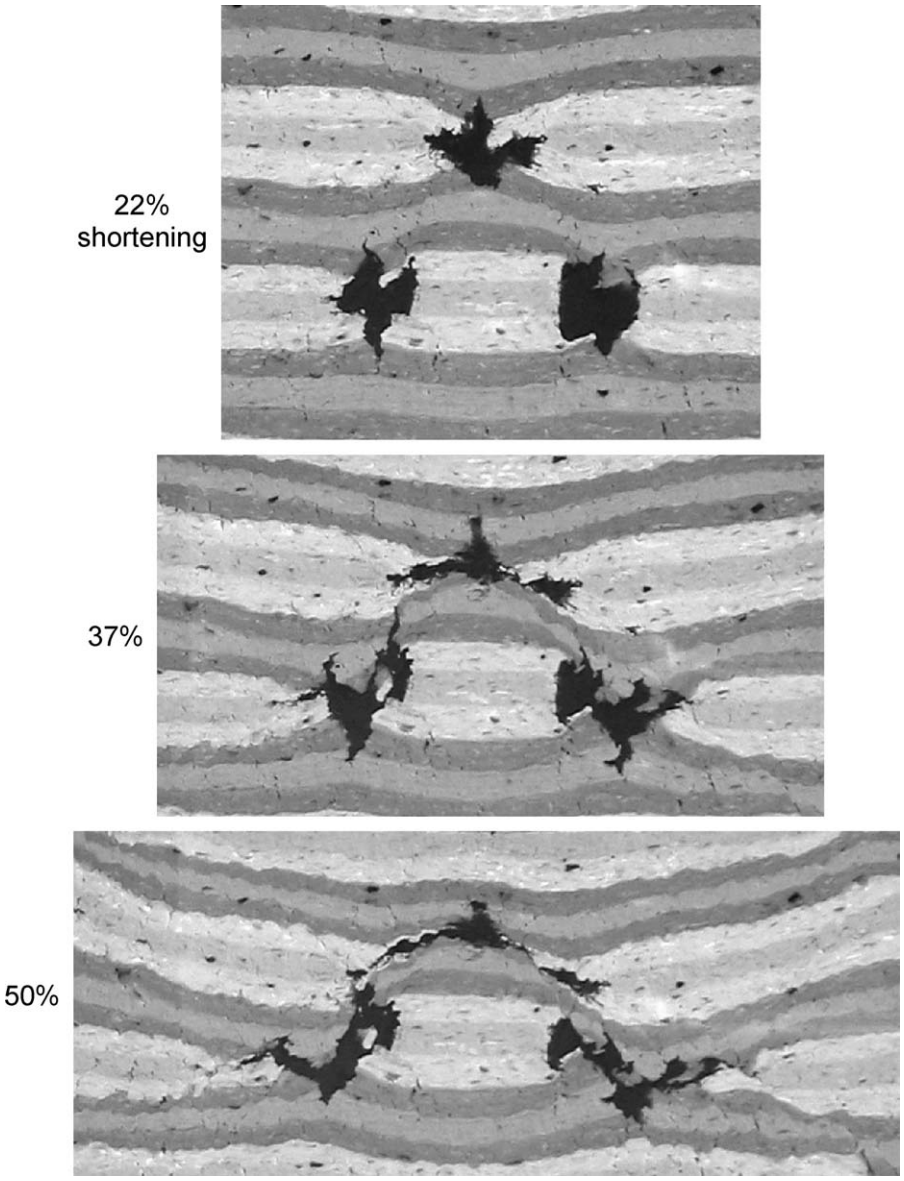

Fig. 9. Photographs of three deformation stages of an experiment performed under layer normal shortening and low cooling rate. Notice the escape of chocolate through tension cracks and larger shear bands.

performed at an intermediate cooling rate. First, chocolate bodies are flattened in the XY plane and a set of small radial cracks form in the high anisotropic layers around chocolate inclusions, which are filled with the chocolate itself. At about 20% shortening, a foliation necking effect is perfectly visible while flattening and crack propagation around molten chocolate proceeds. The resulting structures are analogous to those observed at Cap de Creus and characterized by: (i) irregular, spider-like (Wegmann, 1965) melt patches; and (ii) apparent boudinage of the high anisotropic layers that embed the melt patches. Apparent boudins clearly die-out with distance from the melt patches, the last resembling melt-filled interboudin necks. Between 40% and 50% shortening, the reversal in viscosity contrast between chocolate and plasticine mixture is attained. Then, there is a halt in foliation necking and chocolate deforms in the solid state, stretches at a lower rate than plasticine layers and may even boudinage.

In the experiments performed at lower cooling rates all deformation takes place at the molten stage of chocolate, i.e. chocolate does not solidify. A significant difference with regard to the high-temperature structures developed at the intermediate cooling rate is that for lower cooling rates the foliation necking effect evolves towards tension cracks and discrete shear bands through which molten chocolate migrates. In these situations, different melt patches are interconnected throughout the new fracture pattern which also cross-cuts the white low anisotropic layers (Fig. 9).

Finally, fast cooling experiments give rise to a completely different deformation history and also different finite structures compared to those developed in slow cooling experiments (Fig. 10). In this set of experiments, reversal of viscosity contrast is attained at 20–25% bulk shortening, with chocolate first deforming as a weak inclusion (stretching at a higher rate than plasticine layers). The circular sectional

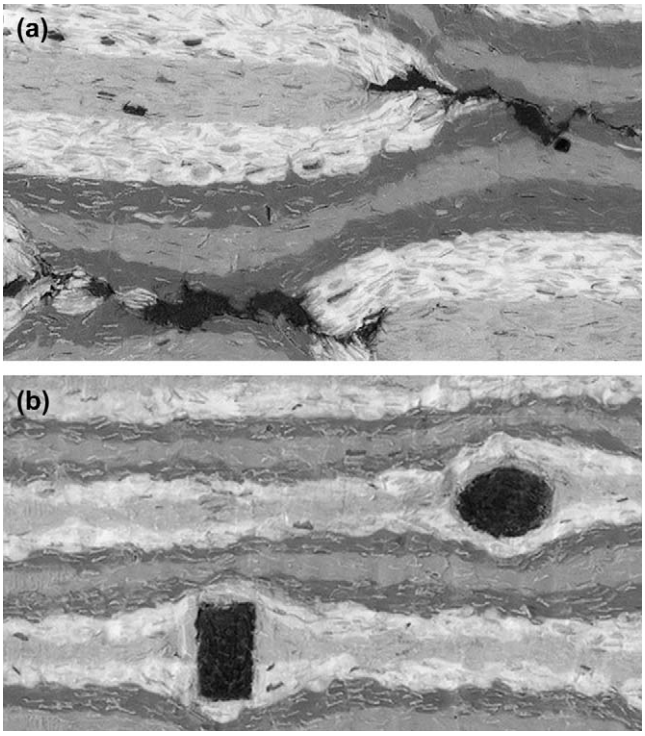

Fig. 10. Details of internal sections of two initially identical specimens deformed up to a 50% layer normal shortening and (a) at a low rate of cooling and (b) at a high rate of cooling. Notice the development of foliation necking in (a) and foliation wrapping effect in (b).

shapes of the initial chocolate inclusions develop into elliptical shapes, whereas the rectangular shapes, initially oriented with their long axes parallel to the shortening axis *Z*, experience a decrease in aspect ratio. After the reversal of viscosity contrast, chocolate behaves rigidly with respect to the surrounding layers, so that solid-state finite structures prevail over molten-state ones and are characterized by the development of a foliation wrapping effect (Fig. 10b).

4.2. Experiments under layer/foliation parallel shortening

These experiments also show the effects of strain localization around crystallizing material. In these cases, during deformation of molten chocolate, tension cracks parallel to foliation/layering nucleate in the plasticine layers adjacent to melt inclusions, and these are subsequently filled with chocolate, developing into chocolate veins. These veins, together with the chocolate remaining in the initial inclusions become progressively deformed, their initial shapes (circles and rectangles) being modified into irregular, patchy lenses. Deformation of the enclosing plasticine layers is controlled by chocolate inclusions during the whole experiment, with folds nucleating around them (Fig. 11b). Folds are disharmonic, showing large variation in axial plane orientation, wavelength and amplitude both at molten and solid states. It is inferred that the irregular fold patterns are imposed by the irregular melt patches. These folds have similarities with the "viscous folds" described by McLellan (1984) as typically developed in partially molten systems.

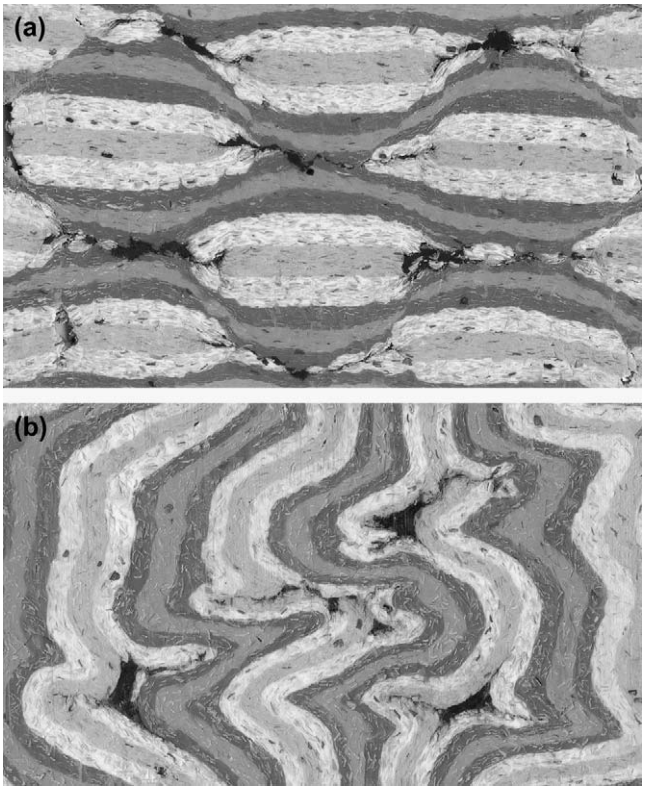

Fig. 11. Photographs of internal sections of two model specimens after (a) 50% layer normal shortening and (b) 50% layer parallel shortening, both performed at a intermediate cooling rate (see text for further description).

5. Discussion

The results of analogue models have many similarities with the structures observed in migmatite terrains at Cap de Creus. Information from both natural and experimental syntectonic migmatites has been integrated, and their significance and main implications will be treated in the following discussion.

5.1. Role of melt in strain localization

The natural and experimental examples shown in this work evidence the strong influence of melt in strain localization. Thus, these can be added to other indicators of melt-enhanced deformation reported in the literature (McLellan, 1984; Davidson et al., 1994; Brown and Solar, 1998; Grujic and Mancktelow, 1998; Mancktelow, 2002). In these experiments, the necking of layering/anisotropy around melt accumulations is the most distinctive structure developed before cooling of the melt phase. These structures are geometrically similar to the boudin neck-like structures observed at Cap de Creus. Foliation necking effect develops if the molten material stretches faster than the embedding layer, regardless of the ratio of stretching between different layers. As demonstrated experimentally, the presence in anatectic areas of necking structures around leucosomes does not necessarily imply that the leucosomes fill interboudin partitions. It could instead be the result of an opposite effect, with boudinage-like structures localizing in sites of melt accumulation. This has implications for

tectonic interpretations of anatectic areas due to strain overestimations or erroneous structural analysis that would derive from the assumption of boudinage. To avoid incorrect interpretations particular attention should be paid to those cases where the foliation necking effect could apply, i.e. where leucosomes are developed in fertile pelitic layers and/or where equivalent undeformed patches are preserved.

In addition, foliation necking effect may be enhanced by extension parallel to layer/foliation, as observed in the experiments under layer normal shortening and inferred from the Cap de Creus structures, or, as deduced from other natural migmatite structures, may also be favoured by volume loss due to melt extraction (Bons, 1999). The strong control of melt pods in strain localization is persistent in the experiments performed at low cooling rates, in which the foliation necking effect is followed by the development of discrete shear bands interconnecting adjacent leucosomes. Grujic and Mancktelow (1998) and Mancktelow (2002) have already demonstrated that conjugate shear domains nucleate on weak inclusions and that they link up to form anastomosing networks of high strain domains.

Whereas boudin neck-like structures and shear bands are typical results of strain localization around melt patches under layer normal shortening, the equivalent effect under layer parallel shortening is the folding of the anisotropic layers. As described before, fold geometries reflect a strong melt phase control on fold nucleation and evolution, as any small inclusion of molten material will act as an instability which triggers folding of the layers.

5.2. Reversal of rheological contrast

A unique feature of the experiments presented here is that they include the effects of phase transition and changing rheology of the inclusions (patches) during deformation. The effective viscosity ratio between inclusions and layered matrix becomes inverse in a small temperature interval. This is thought to occur in syntectonic migmatites involving a crystallizing leucosome and a gneissic or schistose mesosome.

As stated before, deformation tends to localize around the melt-bearing phase, and, as also shown in these experiments, continues developing around the solid leucosomes after their crystallization. This gives rise to the development of a range of structures that can be correlated with different mechanical behaviours of migmatites, with a rheological threshold marked by the reversal of competence contrast between leucosome and host rock. Fig. 12 illustrates a model deduced from the combination of field and experimental data to explain the

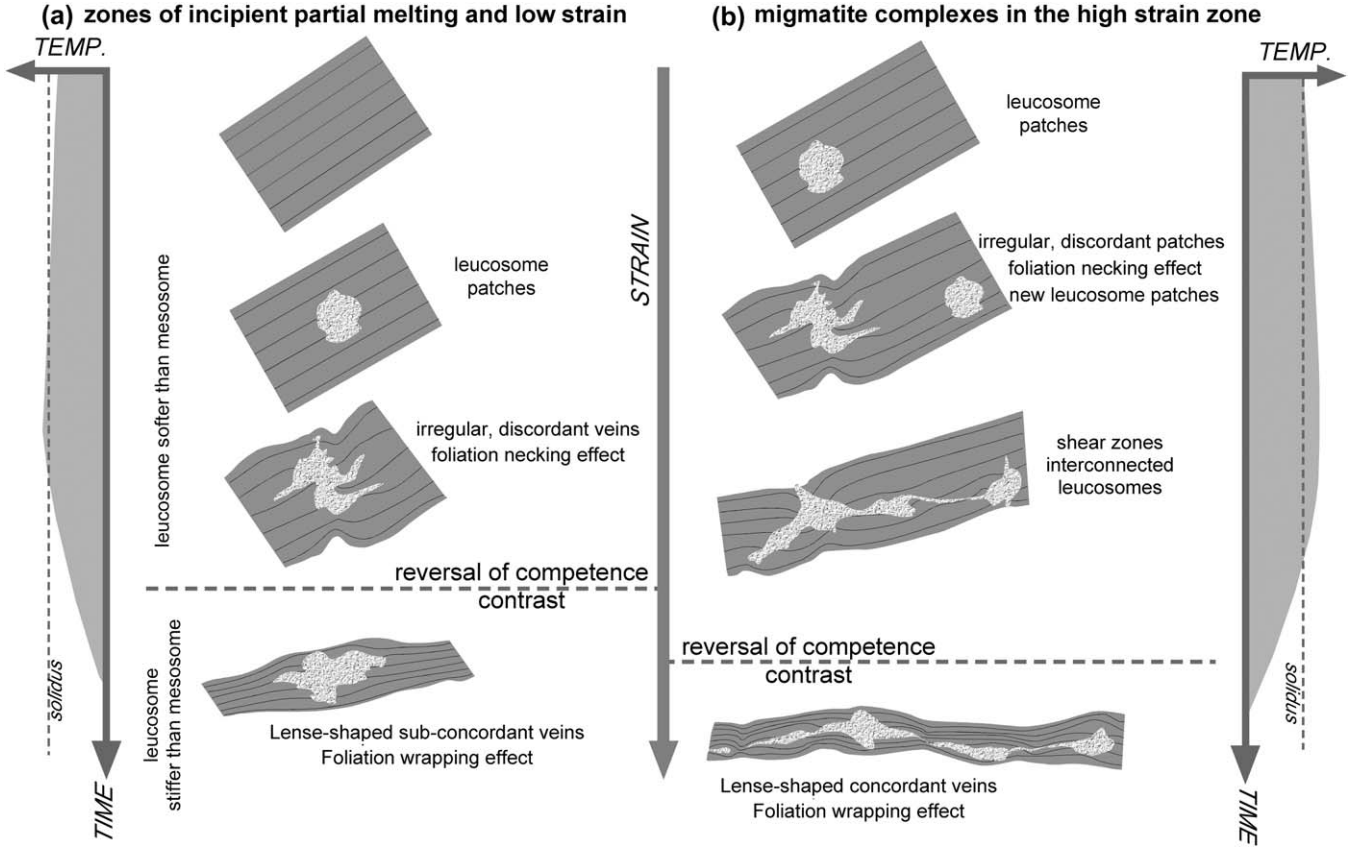

Fig. 12. Idealized sketch of a model for the development of syntectonic leucosomes and related structures based on field observations at Cap de Creus and experimental results. Qualitative relations between time, temperature and strain are shown. During regional deformation, initial melt-bearing pods (formed in pelitic layers) evolve towards irregular patches and lensoid veins. (a) and (b) refer to two areas with rather different tectonothermal evolution. (a) Structural evolution in domains of incipient partial melting and low strain. (b) Structural evolution in anatectic domains of high strain. The model is applicable to the Cap de Creus area and potentially to other migmatitic zones.

deformational evolution of syntectonic migmatites. Before full crystallization, the leucosome is much softer than the mesosome (Table 1) and foliation necking patterns develop at their interphase. With progressive deformation, initial melt inclusions (preferentially formed in pelitic layers) develop into irregular, discordant patches, with veins emanating from the partially melted inclusions (Fig. 12). After full crystallization, the leucosome becomes stiffer than the mesosome and the foliated mesosome wraps around the veins. This foliation wrapping effect may partially or completely overprint the previous necking patterns. With regard to the inclusions, the irregular patches continue deforming in the solid state to form elongate lenses sub-concordant with layering or foliation and, since they are stiffer than matrix, they may be folded or boudinaged. Incorrect assumptions concerning the initial sheet-like shape of leucosomes may lead to errors in estimation of strain from deformed migmatites.

The reversal of rheological contrast and its consequences in terms of deformational behaviour are thought to be easily extrapolated to magmatic veins and dykes intruded in mid to low crustal domains.

5.3. Role of tectonothermal history

The here presented experimental studies show that, under a constant bulk strain rate, the thermal history has a strong influence on the structural development of syntectonic migmatites. In particular, the role of the cooling rate has been investigated. In the experiments performed under rapid temperature drop, most deformation occurs after the molten phase has solidified and thus solid-state structures prevail. On the contrary, experiments subjected to a slow temperature drop show the dominance of structures developed at the molten stage of leucosomes.

On the other hand, migmatite structures from Cap de Creus reveal that deformation and migmatization processes were spatially and temporally related. Fig. 12 summarizes these relationships and integrates to some extent the field evidence and experimental results. Domains of relative low strain and low temperature are characterized by the presence of isolated leucosome patches, with foliation necking patterns preserved or weakly overprinted by late solid-state deformation (Fig. 12a). In contrast, migmatites that are restricted to domains of relative high strain and pervasive partial melting (migmatite complexes) exhibit distinct structural patterns. There, since higher temperatures were likely achieved, partial melts would have remained longer in the system, several leucosome generations would form and reversal of competence contrast would have been attained later (Fig. 12b), compared to the zones of incipient partial melting. Furthermore, high strain and high temperature conditions would enable the development of shear zones and melt migration along them, similar to the situation observed in the experiments performed at low cooling rate. The latest generations of leucosomes would record the smallest amount of deformation in the partially molten stage, rapidly deforming in the solid state (Fig. 12b) as the situation observed in the experiments performed at high cooling rate.

6. Conclusions

In high grade crustal domains of coeval deformation and partial melting, deformation tends to localize around syntectonic melts, giving rise to a range of particular structures that can be correlated with different rheological stages of leucosomes, with a rheological threshold marked by the reversal of competence contrast between the leucosome and host rock. This has been investigated by means of field studies and experimental modelling. The experimental results show that the reversal of viscosity contrast is associated with an increase in effective viscosity of the leucosomes due to crystallization. The similarity and coherence between natural and analogue migmatite structures proves that chocolate is a good analogue of crystallizing melt at the meso- (and macro-) scale.

The common presence in anatectic areas of foliation/layering deflections around leucosome patches or veins does not necessarily imply that melt filled boudin necks or extensional fractures, but it could be the result of an opposite effect: boudinage-like structures localized in sites of melt accumulation, with consequent implications for strain estimations in migmatite terrains.

Acknowledgements

This article is dedicated to the memory of Elena's parents, deceased in 2005. We wish to thank Y.-T. Takeda, P.D. Bons and A. Griera for helpful discussions on various aspects related to this work, and to L.M. Castaño, and again to A. Griera and Y.-T. Takeda for laboratory support. We gratefully acknowledge M. Brown and S. Sengupta, whose constructive reviews greatly improved the manuscript. Many thanks to I. Alsop for helpful comments and English corrections. This work was financed by the Spanish Ministry of Education and Science (projects BTE2001-2616 and CGL2004-03657/BTE).

References

Arzi, A.A., 1978. Critical phenomena in the rheology of partially melted rocks. Tectonophysics 44, 173–184.

Barnes, H.A., 1999. The yield stress—a review or "panta rei" – everything flows? Journal of Non-Newtonian Fluid Mechanics 81, 133–178.

Barraud, J., Gardien, V., Allemand, P., Grandjean, P., 2004. Analogue models of melt-flow networks in folding migmatites. Journal of Structural Geology 26, 307–324.

Beckett, S.T., 2000. The Science of Chocolate. Royal Society of Chemistry, Cambridge.

Benn, K., Cruden, A.R., Sawyer, E.W., (Eds.) 1998. Extraction, transport and emplacement of granitic magmas. Journal of Structural Geology 20 (9–10).

Bons, P.D., 1999. Apparent extensional structures due to volume loss. Proceedings of the Estonian Academy of Sciences 48, 3–14.

Bons, P.D., Elburg, M.A., Dougherty-Page, J., 2001. Analogue modelling of segregation and ascent of magma. Journal of the Virtual Explorer 4, 7–14.

Bons, P.D., Druguet, E., Hamann, I., Carreras, J., Passchier, C.W., 2004. Apparent boudinage in dykes. Journal of Structural Geology 26, 625–636.

Bouchez, J.L., Hutton, D.H.W., Stephens, W.E. (Eds.), 1997. Granite: From Segregation of Melt to Emplacement Fabrics. Kluwer Academic Publishers, Dordrecht.

Brown, M., 1994. The generation, segregation, ascent and emplacement of granite magma: the migmatite-to-crustally-derived granite connection in thickened orogens. Earth Sciences Reviews 36, 83–130.

Brown, M., 2004. The mechanism of melt extraction from lower continental crust of orogens. Transactions of the Royal Society of Edinburgh: Earth Sciences 95, 35–48.

Brown, M., Solar, G.S., 1998. Shear-zone systems and melts: feedback relations and self-organization in orogenic belts. Journal of Structural Geology 20, 211–227.

Brown, M., Solar, G.S., 1999. The mechanism of ascent and emplacement of granite magma during transpression: a syntectonic granite paradigm. Tectonophysics 312, 1–33.

Carreras, J., Julivert, M., Soldevila, A., Griera, A., Soler, D., 2000a. A deformation stage for analogue modelling of structures developed under variable degree of non-coaxiality. Geoscience 2000. University of Manchester, Abstracts volume, section Modelling in Structural Geology, p. 126.

Carreras, J., Druguet, E., Griera, A., 2000b. Desarrollo de zonas de cizalla conjugadas por deformación coaxial de materiales analógicos anisótropos. Geotemas 1, 47–52.

Castro, A., Fernández, S., Vigneresse, J.L., 1999. Understanding granites: integrating new and classical techniques. Special Publication – Geological Society of London 168.

Davidson, C., Schmid, S.M., Hollister, L.S., 1994. Role of melt during deformation in the deep crust. Terra Nova 6, 133–142.

D'Lemos, R.S., Brown, M., Strachan, R.A., 1992. Granite magma generation, ascent and emplacement within a transpressional orogen. Journal of the Geological Society, London 149, 487–490.

Druguet, E., 2001. Development of high thermal gradients by coeval transpression and magmatism during the Variscan orogeny: insights from the Cap de Creus (Eastern Pyrenees). Tectonophysics 332, 275–293.

Druguet, E., Hutton, D.H.W., 1998. Syntectonic anatexis and magmatism in a mid-crustal transpressional shear zone: an example from the Hercynian rocks of the Eastern Pyrenees. Journal of Structural Geology 20, 905–916.

Druguet, E., Enrique, P., Galán, G., 1995. Tipología de los granitoides y las rocas asociadas del complejo migmatítico de la Punta dels Farallons (Cap de Creus, Pirineo Oriental). Geogaceta 18, 199–202.

Druguet, E., Passchier, C.W., Carreras, J., Victor, P., den Brok, S.W.J., 1997. Analysis of a complex high-strain zone at Cap de Creus, Spain. Tectonophysics 280, 31–45.

Galland, O., de Bremond d'Ars, J., Cobbold, P.R., Hallot, E., 2003. Physical models of magmatic intrusion during thrusting. Terra Nova 15, 405–409.

Ghosh, S.K., Sengupta, S., 1999. Boudinage and composite boudinage in superposed deformations and syntectonic migmatization. Journal of Structural Geology 21, 97–110.

Gómez-Rivas, E., Carreras, J., Druguet, E., Griera, A., 2005. Analogue Modelling of the Development of Shear Bands in Foliated Materials Under Coaxial Deformation. 15th Conference on Deformation Mechanisms, Rheology and Tectonics, ETH Zurich. Abstract volume, p. 91.

Grujic, D., Mancktelow, N.S., 1998. Melt-bearing shear zones: analogue experiments and comparison with examples from southern Madagascar. Journal of Structural Geology 20, 673–680.

Hollister, L.S., Crawford, M.L., 1986. Melt-enhanced deformation: a major tectonic process. Geology 14, 558–561.

Hutton, D.H.W., 1988. Granite emplacement mechanisms and tectonic controls: inferences from deformation studies. Transactions of the Royal Society of Edinburgh: Earth Sciences 79, 245–255.

Kisters, A.F.M., Gibson, R.L., Charlesworth, E.G., Anhaeusser, C.R., 1998. The role of strain localization in the segregation and ascent of anatectic melts, Namaqualand, South Africa. Journal of Structural Geology 20, 229–242.

Kovac, J., 2002. The science of chocolate (by Stephen T. Beckett). Journal of Chemical Education 79, 167.

Labrousse, L., Jolivet, L., Agard, P., Hébert, R., Andersen, T.B., 2002. Crustal-scale boudinage and migmatization of gneiss during their exhumation in the UHP Province of Western Norway. Terra Nova 14, 263–270.

Lacassin, R., 1988. Large-scale foliation boudinage in gneisses. Journal of Structural Geology 10, 643–647.

Mancktelow, N.S., 2002. Finite-element modelling of shear zone development in viscoelastic materials and its implications for localisation of partial melts. Journal of Structural Geology 24, 1045–1053.

Marchildon, N., Brown, M., 2003. Spatial distribution of melt-bearing structures in anatectic rocks from Southern Brittany, France: implications for melt transfer at grain- to orogen-scale. Tectonophysics 364, 215–235.

McClay, K.R., 1976. The rheology of plasticine. Tectonophysics 33, T7–T15.

McLellan, E.L., 1984. Deformational behaviour of migmatites and problems of structural analysis in migmatite terrains. Geological Magazine 121, 339–345.

McLellan, E.L., 1988. Migmatite structures in the Central Gneis Complex, Boca de Quadra, Alaska. Journal of Metamorphic Geology 6, 517–542.

Means, W.D., Park, Y., 1994. New experimental approach to understanding igneous texture. Geology 22, 323–326.

Park, Y., Means, W.D., 1996. Direct observation of deformation processes in crystal mushes. Journal of Structural Geology 18, 847–858.

Petford, N., 2003. Rheology of granitic magmas during ascent and emplacement. Annual Reviews of Earth and Planetary Sciences 31, 399–427.

Pfiffner, O.A., Ramsay, J.G., 1982. Constraints on geological strain rates: arguments from finite strain states naturally deformed rocks. Journal of Geophysical Research 87, 311–321.

Ramberg, H., 1955. Natural and experimental boudinage and pinch-and-swell structures. Journal of Geology 63, 512–526.

Ramberg, H., 1967. Gravity, Deformation and the Earth's Crust, as Studied by Centrifuged Models. Academic Press, London.

Ramírez, J., 1983. Els gneiss de Port de la Selva: Significació petrològica i relacions amb l'encaixant. M.Sc. thesis, University of Barcelona.

Román-Berdiel, T., Gapais, D., Brun, J.-P., 1997. Granite intrusion along strike-slip zones in experiment and nature. American Journal of Science 297, 651–678.

Rosenberg, C.L., Handy, M.R., 2000. Syntectonic melt pathways during simple shearing of a partially-molten rock analogue (norcamphor-benzamide). Journal of Geophysical Research 105, 3135–3149.

Rosenberg, C.L., Handy, M.R., 2005. Experimental deformation of partially melted granite revisited: implications for the continental crust. Journal of Metamorphic Geology 23, 19–28.

Shackleton, M.E., Green, R.G., 1993. On-line viscometer for measurement in the range 1 to 100 Pa s. Measurement Science and Technology 4, 395–404.

Swanson, M.T., 1992. Late Acadian-Alleghenian transpressional deformation: evidence from asymmetric boudinage in the Casco Bay area, coastal Maine. Journal of Structural Geology 14, 323–341.

Vanderhaeghe, O., 1999. Pervasive melt migration from migmatites to leucogranite in the Shuswap metamorphic core complex, Canada: control of regional deformation. Tectonophysics 312, 35–55.

Vernon, R.H., Collins, W.J., Richards, S.W., 2003. Contrasting magmas in metapelitic and metapsammitic migmatites in the Cooma Complex, Australia. Visual Geosciences 8, 45–54.

Walte, N.P., Bons, P.D., Passchier, C.W., 2005. Deformation of melt-bearing systems – insight from in situ grain-scale analogue experiments. Journal of Structural Geology 27, 1666–1679.

Wegmann, C.E., 1965. Tectonic patterns at different levels. Geological Society of South Africa 66, 1–78. Annexure (Du Toit memorial lecture 8).

Zulauf, J., Zulauf, G., 2004. Rheology of plasticine used as rock analogue: the impact of temperature, composition and strain. Journal of Structural Geology 26, 725–737.